

UC Santa Cruz

UC Santa Cruz Previously Published Works

Title

Globally, tree fecundity exceeds productivity gradients

Permalink

<https://escholarship.org/uc/item/16j80763>

Journal

Ecology Letters, 25(6)

ISSN

1461-023X

Authors

Journé, Valentin
Andrus, Robert
Aravena, Marie-Claire
[et al.](#)

Publication Date

2022-06-01

DOI

10.1111/ele.14012

Peer reviewed

Globally, tree fecundity exceeds productivity gradients

Valentin Journé,¹ Robert Andrus,² Marie-Claire Aravena,³ Davide Ascoli,⁴ Roberta Berretti,⁴ Daniel Berveiller,⁵ Michal Bogdziewicz,⁶ Thomas Boivin,⁷ Raul Bonal,⁸ Thomas Caignard,⁹ Rafael Calama,¹⁰ J. Julio Camarero,¹¹ Chia-Hao Chang-Yang,¹² Benoit Courbaud,¹ Francois Courbet,⁷ Thomas Curt,¹³ Adrian J. Das,¹⁴ Evangelia Daskalidou,¹⁵ Hendrik Davi,⁷ Nicolas Delapierre,⁵ Sylvain Delzon,⁹ Michael Dietze,¹⁶ Sergio Donoso Calderon,³ Laurent Dormont,¹⁷ Josep Maria Espelta,¹⁸ Timothy J. Fahey,¹⁹ William Farfan-Rios,²⁰ Catherine A. Gehring,²¹ Gregory S. Gilbert,²² Georg Gratzer,²³ Cathryn H. Greenberg,²⁴ Qinfeng Guo,²⁵ Andrew Hackett-Pain,²⁶ Arndt Hampe,⁹ Qingmin Han,²⁷ Janneke Hille Ris Lambers,²⁸ Kazuhiko Hoshizaki,²⁹ Ines Ibanez,³⁰ Jill F. Johnstone,³¹ Daisuke Kabeya,²⁷ Roland Kays,³² Thomas Kitzberger,³³ Johannes M.H. Knops,³⁴ Richard K. Kobe,³⁵ Georges Kunstler,¹ Jonathan G.A. Lageard,³⁶ Jalene M. LaMontagne,³⁷ Theodor Leininger,³⁸ Jean-Marc Limousin,³⁹ James A. Lutz,⁴⁰ Diana Macias,⁴¹ Eliot J.B. McIntire,⁴² Christopher M. Moore,⁴³ Emily Moran,⁴⁴ Renzo Motta,⁴ Jonathan A. Myers,⁴⁵ Thomas A. Nagel,⁴⁶ Kyotaro Noguchi,⁴⁷ Jean-Marc Ourcival,³⁹ Robert Parmenter,⁴⁸ Ian S. Pearse,⁴⁹ Ignacio M. Perez-Ramos,⁵⁰ Lukasz Piechnik,⁵¹ John Poulsen,⁵² Renata Poulton-Kamakura,⁵² Tong Qiu,⁵² Miranda D. Redmond,⁵³ Chantal D. Reid,⁵² Kyle C. Rodman,⁵⁴ Francisco Rodriguez-Sanchez,⁵⁵ Javier D. Sanguinetti,⁵⁶ C. Lane Scher,⁵² Harald Schmidt Van Marle,³ Barbara Seget,⁵¹ Shubhi Sharma,⁵² Miles Silman,⁵⁷ Michael A. Steele,⁵⁸ Nathan L. Stephenson,¹⁴ Jacob N. Straub,⁵⁹ Jennifer J. Swenson,⁵² Margaret Swift,⁵² Peter A. Thomas,⁶⁰ Maria Uriarte,⁶¹ Giorgio Vacchiano,⁶² Thomas T. Veblen,² Amy V. Whipple,⁶³ Thomas G. Whitham,⁶³ Boyd Wright,⁶⁴ S. Joseph Wright,⁶⁵ Kai Zhu,²² Jess K. Zimmerman,⁶⁶ Roman Zlotin,⁶⁷ Magdalena Zywiec,⁵¹ and James S. Clark,^{1,52}

¹Universite Grenoble Alpes, Institut National de Recherche pour Agriculture, Alimentation et Environnement (INRAE), Laboratoire EcoSystemes et Societes En Montagne (LESSEM), 38402 St. Martin-d'Herès, France.

²Department of Geography, University of Colorado Boulder, Boulder, CO 80309 USA.

³Universidad de Chile, Facultad de Ciencias Forestales y de la Conservacion de la Naturaleza (FCFCN), La Pintana, 8820808 Santiago, Chile.

⁴Department of Agriculture, Forest and Food Sciences, University of Torino, 10095 Grugliasco, TO, Italy.

⁵Universite Paris-Saclay, Centre national de la recherche scientifique, AgroParisTech, Ecologie Systematique et Evolution, 91405 Orsay, France.

⁶Department of Systematic Zoology, Faculty of Biology, Adam Mickiewicz University, Umultowska 89, 61-614 Poznan, Poland.

⁷Institut National de Recherche pour Agriculture, Alimentation et Environnement (INRAE), Ecologie des Forets Mediterranennes, 84000 Avignon, France.

⁸Department of Biodiversity, Ecology and Evolution, Complutense University of Madrid, 28040 Madrid, Spain.

⁹Universite Bordeaux, Institut National de Recherche pour Agriculture, Alimentation et Environnement (INRAE), Biodiversity, Genes, and Communities (BIOGECO), 33615 Pessac, France.

¹⁰Centro de Investigacion Forestal (INIA-CSIC), 28040 Madrid, Spain .

¹¹Instituto Pirenaico de Ecologia, Consejo Superior de Investigaciones Cientificas (IPE-CSIC), 50059 Zaragoza, Spain.

¹²Department of Biological Sciences, National Sun Yat-sen University, Kaohsiung 80424, Taiwan.

42 ¹³Aix Marseille universite, Institut National de Recherche pour Agriculture, Alimentation et Environnement (IN-
43 RAE), 13182 Aix-en-Provence, France.

44 ¹⁴USGS Western Ecological Research Center, Three Rivers, CA, 93271 USA.

45 ¹⁵Institute of Mediterranean and Forest Ecosystems, Hellenic Agricultural Organization DEMETER, 11528 Athens,
46 Greece.

47 ¹⁶Earth and Environment, Boston University, Boston, MA, 02215 USA.

48 ¹⁷Centre d'Ecologie Fonctionnelle et Evolutive (CEFE), Centre National de la Recherche Scientifique (CNRS),
49 34293 Montpellier, France..

50 ¹⁸Centre de Recerca Ecologica i Aplicacions Forestals (CREAF), Bellaterra, Catalunya 08193, Spain.

51 ¹⁹Natural Resources, Cornell University, Ithaca, NY, 14853 USA.

52 ²⁰Washington University in Saint Louis, Center for Conservation and Sustainable Development, Missouri Botanical
53 Garden, St. Louis, MO 63110 USA.

54 ²¹Department of Biological Sciences and Center for Adaptive Western Landscapes.

55 ²²Department of Environmental Studies, University of California, Santa Cruz, CA 95064 USA.

56 ²³Institute of Forest Ecology, Peter-Jordan-Strasse 82, 1190 Wien, Austria.

57 ²⁴Bent Creek Experimental Forest, USDA Forest Service, Asheville, NC 28801 USA.

58 ²⁵Eastern Forest Environmental Threat Assessment Center, USDA Forest Service, Southern Research Station,
59 Research Triangle Park, NC 27709 USA.

60 ²⁶Department of Geography and Planning, School of Environmental Sciences, University of Liverpool, Liverpool,
61 United Kingdom.

62 ²⁷Department of Plant Ecology Forestry and Forest Products Research Institute (FFPRI), Tsukuba, Ibaraki, 305-
63 8687 Japan.

64 ²⁸Department of Environmental Systems Science, ETH Zurich, Switzerland 8092.

65 ²⁹Department of Biological Environment, Akita Prefectural University, Akita 010-0195, Japan.

66 ³⁰School for Environment and Sustainability, University of Michigan, Ann Arbor, MI 48109.

67 ³¹Institute of Arctic Biology, University of Alaska, Fairbanks, AK 99700, USA.

68 ³²Department of Forestry and Environmental Resources, NC State University, Raleigh, NC USA.

69 ³³Department of Ecology, Instituto de Investigaciones en Biodiversidad y Medioambiente (Consejo Nacional de
70 Investigaciones Científicas y Técnicas - Universidad Nacional del Comahue), Quintral 1250, 8400 Bariloche, Ar-
71 gentina.

72 ³⁴Health and Environmental Sciences Department, Xian Jiaotong-Liverpool University, Suzhou, China, 215123.

73 ³⁵Department of Plant Biology, Program in Ecology, Evolutionary Biology, and Behavior, Michigan State Univer-
74 sity, East Lansing, MI 48824.

75 ³⁶Department of Natural Sciences, Manchester Metropolitan University, Manchester M1 5GD, UK.

76 ³⁷Department of Biological Sciences, DePaul University, Chicago, IL 60614 USA.

77 ³⁸USDA, Forest Service, Southern Research Station, PO Box 227, Stoneville, MS 38776.

78 ³⁹CEFE, Univ Montpellier, CNRS, EPHE, IRD, 1919 route de Mende, 34293 Montpellier Cedex 5, France.

79 ⁴⁰Department of Wildland Resources, and the Ecology Center, Utah State University, Logan, UT 84322 USA.

80 ⁴¹Department of Biology, University of New Mexico, Albuquerque, NM 87131 USA.

81 ⁴²Pacific Forestry Centre, Victoria, British Columbia, V8Z 1M5 Canada.

82 ⁴³Department of Biology, Colby College, Waterville, ME 04901 USA.

83 ⁴⁴School of Natural Sciences, UC Merced, Merced, CA 95343 USA.

84 ⁴⁵Department of Biology, Washington University in St. Louis, St. Louis, MO.

85 ⁴⁶Department of forestry and renewable forest resources, Biotechnical Faculty, University of Ljubljana, Ljubljana,
86 Slovenia.

87 ⁴⁷Tohoku Research Center, Forestry and Forest Products Research Institute, Morioka, Iwate, 020-0123, Japan.

88 ⁴⁸Valles Caldera National Preserve, National Park Service, Jemez Springs, NM 87025 USA.

89 ⁴⁹Fort Collins Science Center, 2150 Centre Avenue, Bldg C, Fort Collins, CO 80526 USA.

90 ⁵⁰Inst. de Recursos Naturales y Agrobiología de Sevilla, Consejo Superior de Investigaciones Científicas (IRNAS-
91 CSIC), Seville, Andalucía, Spain.

92 ⁵¹W. Szafer Institute of Botany, Polish Academy of Sciences, Lubicz 46, 31-512 Krakow, Poland.

93 ⁵²Nicholas School of the Environment, Duke University, Durham, NC 27708 USA.

94 ⁵³Department of Forest and Rangeland Stewardship, Colorado State University, Fort Collins, CO, USA.

95 ⁵⁴Department of Forest and Wildlife Ecology, University of Wisconsin-Madison, Madison, WI 53706 USA.

96 ⁵⁵Department of Biología Vegetal y Ecología, Universidad de Sevilla, 41012 Sevilla, Spain.

97 ⁵⁶Bilogo Dpto. Conservación y Manejo Parque Nacional Lanín Elordi y Perito Moreno 8370, San Martín de los
98 Andes Neuquén Argentina.

99 ⁵⁷Department of Biology, Wake Forest University, 1834 Wake Forest Rd, Winston-Salem, NC 27106 USA.

100 ⁵⁸Department of Biology, Wilkes University, 84 West South Street, Wilkes-Barre, PA 18766 USA.

101 ⁵⁹Department of Environmental Science and Ecology, State University of New York-Brockport, Brockport, NY
102 14420 USA.

103 ⁶⁰School of Life Sciences, Keele University, Staffordshire ST5 5BG, UK.

104 ⁶¹Department of Ecology, Evolution and Environmental Biology, Columbia University, 1113 Schermerhorn Ext.,
105 1200 Amsterdam Ave., New York, NY 10027.

106 ⁶²Department of Agricultural and Environmental Sciences - Production, Territory, Agroenergy (DISAA), Univer-
107 sity of Milan, 20133 Milano, Italy.

108 ⁶³Department of Biological Sciences, Northern Arizona University, Flagstaff, AZ 86011 USA.

109 ⁶⁴Botany, School of Environmental and Rural Science, University of New England, Armidale, NSW, 2350, Aus-
110 tralia.

111 ⁶⁵Smithsonian Tropical Research Institute, Apartado 0843n03092, Balboa, Republic of Panama.

112 ⁶⁶Department of Environmental Sciences, University of Puerto Rico, Río Piedras, PR 00936 USA.

113 ⁶⁷Geography Department and Russian and East European Institute, Bloomington, IN 47405 USA

114

115

116 *keywords:* climate | competition | forest regeneration | seed consumption | species interactions
117 | tree fecundity

118

119 **Short running title:** Global trends in tree fecundity

120

121 *Type of article:* Letter #Total word count abstract: 132 #Total word count main text: ~ 3900
122 #Total word count figure legends: ~ 500 # 67 references # 0 Table and 6 Figures (color) # 1
123 Supporting information

124

125 **Data availability statement**

126 All data and code supporting our results are archived on the Zenodo Repository at the following
127 link: <https://doi.org/10.5281/zenodo.6381799>

128

129 **Author contributions**

130 V.J. and J.S.C performed analyses and co-wrote the paper, J.S.C. designed the study, compiled
131 the MASTIF network, and wrote the MASTIF model and software, M.B, B.C., G.K, and T.Q.
132 co-wrote the paper, and all authors contributed data and revised the paper.

133

Abstract

Lack of tree fecundity data across climatic gradients precludes analysis of how seed supply contributes to global variation in forest regeneration and biotic interactions responsible for biodiversity. A global synthesis of raw seed-production data shows a 250-fold increase in seed abundance from cold-dry to warm-wet climates, driven primarily by a 100-fold increase in seed production for a given tree size. The modest (three-fold) increase in forest productivity across the same climate gradient cannot explain the magnitudes of these trends. The increase in seeds per tree can arise from adaptive evolution driven by intense species interactions or from the direct effects of a warm, moist climate on tree fecundity. Either way, the massive differences in seed supply ramify through food webs potentially explaining a disproportionate role for species interactions in the wet tropics.

Introduction

Understanding how tree fecundity contributes to global biodiversity and ecosystem function requires estimates of latitudinal trends in seed production. At the community scale, tree fecundity determines the density of competing offspring and the diets of consumers and seed dispersers that depend on seeds and seedlings (Terborgh, 1986; Corlett, 2013; Mokany *et al.*, 2014). Diversity, stem density, and growth and mortality rates all show important trends with latitude (Phillips & Gentry, 1994; Lewis *et al.*, 2004; Stephenson & Van Mantgem, 2005; Chu *et al.*, 2019; Locosselli *et al.*, 2020). Fecundity estimates are now available in North America (Clark *et al.*, 2021; Sharma *et al.*, 2021), but unlike growth and mortality rates (Stephenson & Van Mantgem, 2005; Brienen *et al.*, 2020), fecundity estimates have not been compiled from the tropics. At the global scale, a meta-analysis of 18 seed-trap studies in temperate and tropical forests did not find a relationship between seed-rain density (seeds per area) and latitude, but the same study suggested that seed-mass density might decline with latitude (Moles *et al.*, 2009). If the density of seed mass per-area is higher in the tropics than the temperate zone, does high seed mass density in the tropics come from the fact that tropical trees are simply larger and/or embedded in more productive communities, as assumed in Dynamic Global Vegetation Models (DGVMs) (Sitch *et al.*, 2003; Krinner *et al.*, 2005; Fisher *et al.*, 2018; Hanbury-Brown *et al.*, 2022)? Alternatively, does high seed mass density in the tropics result from greater seed production for a given tree size? Understanding global trends requires estimates of seed-production at both the individual-tree and the per-area scales. We present a new synthesis that allows us to quantify the fecundity gradient on a global scale and determine that the fecundity gradient is amplified in warm/moist climates beyond what can be explained by tree size or NPP.

The global meta-analysis that found a possible trend in seed mass multiplied the number of seeds counted in traps by the average seed size for all plant species that were observed at the same latitude (Moles *et al.*, 2009). Authors recognized the approximate nature of these estimates given the seven-order of magnitude range of seed sizes used to obtain the latitude means. In addition to uncertain seed size, counts from seed traps vary widely depending on precise placement of seed traps relative to locations of trees. Where reproduction is counted directly on trees, studies typically report on one to a few species from one to a few sites, and not seed production for all trees in measured plots, as would be needed to place fecundity on a per-area basis. Recent compilations of year-to-year mast production recognise additional challenges posed by divergent methods, some yielding a range of indices at the individual or stand scale on relativized or ordinal scales (LaMontagne *et al.*, 2020; Pearse *et al.*, 2020). Unlike previous meta-analyses, we analyze raw data referenced to an individual tree-year, i.e., the seed

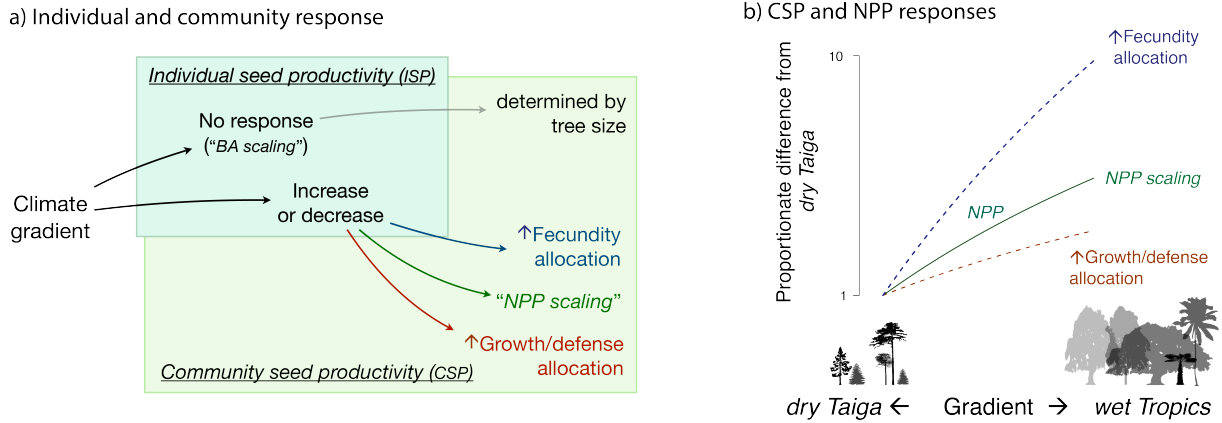


Figure 1: a) Individual seed productivity (ISP, seed mass per tree basal area) might not vary with latitudinal climate gradients, in which case community seed productivity (CSP, seed mass production per forest area) depends on variation in tree size. Alternatively, responses could depend on net primary productivity (NPP), increasing if allocation in warm climates shifts preferentially to fecundity or decreasing if allocation in warm climates shifts to growth and defenses. b) Proportionate differences in fecundity hypothesized for the three scenarios in (a) shown as differences from the climate gradient in NPP. The NPP-scaling scenario means that NPP and CSP follow the same proportionate trajectory (green line).

179 production by each tree in each year, including all trees on inventory plots. By estimating seed
 180 production at the tree-year scale (Clark *et al.*, 2019) we quantify both the trends in individual
 181 production and in the seed production per area.

182 The indicators that we evaluate allow us determine both the gradient in seed productivity of
 183 communities and how the gradient in seed productivity is influenced by individual tree responses.
 184 Individual fecundity could vary due to climate through alternative allocation priorities (Fig. 1a).
 185 Because reproductive effort depends on both seed sizes and numbers (Westoby *et al.*, 1992), and
 186 reproductive effort varies with tree size (Qiu *et al.*, 2021), *individual standardized production*
 187 (ISP) is defined here relative to tree basal area,

$$ISP_{ij} = \frac{\hat{f}_{ijs} \times g_s}{\text{basal area}_i} \quad (1)$$

188 ($\text{g m}^{-2}\text{yr}^{-1}$). ISP depends on the mass of a seed g_s produced by species s and the estimate
 189 of mean seed production \hat{f}_{ijs} for tree i at location j that accounts for effects of shading by
 190 neighbors, and the variation and uncertainty in seed production each year, $f_{ijs,t}$ (see Methods:
 191 [Uncertainty in ISP and CSP](#), eq. (4)). ISP is standardized by tree size to isolate the fecundity
 192 differences that are unrelated to size. If seed production is determined solely by tree size, as
 193 assumed in most ecological models (reviewed in Qiu *et al.* 2021), then climate effects on tree
 194 size still come through the effects of climate on past growth, which, in turn, affects tree size
 195 and thus stand structure; even if trees are larger in the wet tropics, ISP could still be constant
 196 across the climate gradient because ISP is standardized for size. Departures from this constant
 197 response are possible if trees allocate proportionately more or less to fecundity in warm/moist
 198 climates (Fig. 1).

199 While ISP_{ij} can show how individual allocation changes with climate, *community seed*
 200 *production*, CSP_j , quantifies seed production per area of forest, the starting point both for stand
 201 regeneration and the interactions between seeds, seedlings, consumers, and dispersers. [We
 202 hereafter omit subscripts to reduce clutter.] Like NPP, CSP is a community property, defined
 203 as the seed production summed over all trees on a plot and divided by plot area ($\text{g ha}^{-1} \text{yr}^{-1}$,



Figure 2: MASTIF data summary, with symbol size proportional to observations. The distribution of data is detailed in Figure S1 and in Table S1.

204 Methods, eqn 5). CSP might scale as a fraction of NPP, as suggested by some empirical evidence
 205 (Vacchiano *et al.*, 2018) and assumed in DGVMs (Fisher *et al.*, 2018; Hanbury-Brown *et al.*,
 206 2022). NPP scaling predicts high CSP in warm/moist climates where NPP is high (Del Grosso
 207 *et al.*, 2008) (Fig. 1b). It is also possible that intense competition selects for allocation to growth
 208 and defenses that enhance survival. If so, CSP is expected to show a flatter response to climate
 209 than the NPP response to climate ("↑growth/defense in Fig. 1).

210 Alternatively, fecundity responses could be amplified beyond what could be explained by
 211 the effects of climate on size or NPP ("↑fecundity" in Figure 1). There are at least two potential
 212 causes for fecundity amplification, including i) reproductive allocation can respond to favorable
 213 climates because reproduction is unconstrained by the structural and hydraulic constraints that
 214 limit growth responses (Koch *et al.*, 2004; King *et al.*, 2009), and ii) intense species interactions
 215 in the wet tropics amplify selection for reproduction to offset high losses to consumers and
 216 enhance the benefits of frugivory (Terborgh, 1986; Harms *et al.*, 2000; Hille Ris Lambers *et al.*,
 217 2002; Schemske *et al.*, 2009; Levi *et al.*, 2019; Hargreaves *et al.*, 2019).

218 Large data sets are needed to estimate climate effects due to wide variation in seed production.
 219 For a given tree, large crop years often exceed intervening years by orders of magnitude (Mendoza
 220 *et al.*, 2018; Vacchiano *et al.*, 2018; LaMontagne *et al.*, 2020; Koenig, 2021). Variation between
 221 trees also varies by orders of magnitude (Clark *et al.*, 2004; Minor & Kobe, 2019). Seed
 222 production further responds to spatio-temporal variation in habitat and climate (Caignard *et al.*,
 223 2017; Bogdziewicz *et al.*, 2020a), including local competition (Clark *et al.*, 2014, 2019). The
 224 many sources of variation means that biogeographic trends of interest can only be identified
 225 from broad coverage and large sample sizes, while accounting for individual tree condition, local
 226 habitat, and climate (Qiu *et al.*, 2021).

227 This synthesis extends the Masting Inference and Forecasting (MASTIF) network (Clark
 228 *et al.*, 2021; Sharma *et al.*, 2021) to quantify the climate controls on seed production globally
 229 and the extent to which seed-production trends go beyond what can be explained by effects of
 230 tree size and productivity. Data include 12M observations from 147K mature trees and 251
 231 inventory plots (Fig. 2). We summarize climate trends with mean annual temperature and
 232 moisture surplus. Model fitting allows for the effects of individual condition and local habitat
 233 variation by including tree diameter, shade class, and soil cation exchange capacity (CEC), a

234 widely used indicator of soil fertility (Hazelton & Murphy, 2007; Hengl *et al.*, 2017), all of
 235 which affect seed production (Materials and Methods).

236 Material and Methods

237 Fecundity Data

238 This study uses crop-count (CC, on trees) and seed-trap (ST) data (fig. 3) from the [Masting](#)
 239 [Inference and Forecasting \(MASTIF\)](#) project. Most observations (99%) come from longitudinal
 240 studies, where all trees on a plot (ST) or individual trees (CC) are observed repeatedly. Other CC
 241 observations (1%) are obtained opportunistically through the [iNaturalist project MASTIF](#) (Clark
 242 *et al.*, 2019). All observations provide estimates of ISP, including those on isolated trees. CSP
 243 requires seed production from a known area and comes from inventory plots (Table S1). Data
 244 include 12,053,732 tree-year observations from 748 species and 146,744 mature individuals.

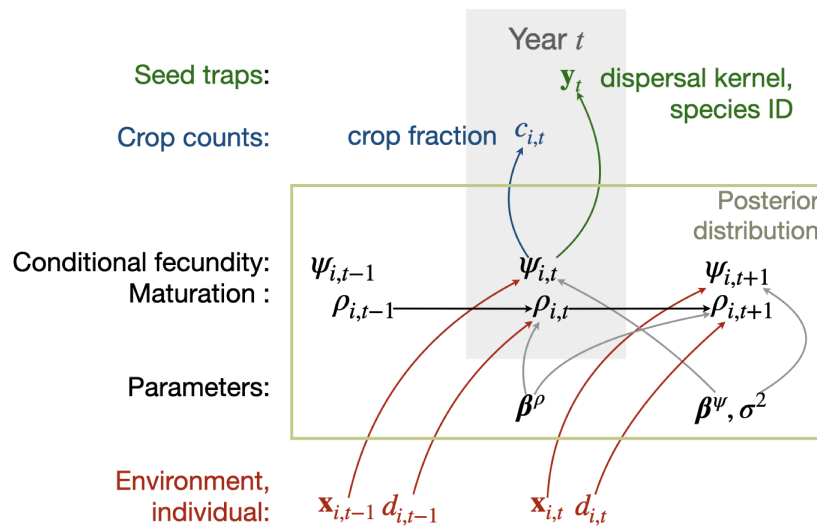


Figure 3: The MASTIF model simplified from Clark *et al.* (2019) to emphasize variables and parameters discussed in the text. A biophysical model for change in fecundity $\psi_{i,t}$ of tree i in year t (a tree-year) is driven by individual tree condition and climate and habitat variables in design vector $\mathbf{x}_{i,t}$ with corresponding coefficients β . Maturation status incorporates tree diameter $d_{i,t}$. The hierarchical state-space model includes process error variance σ^2 and observation error in two data types. A crop count $c_{i,t}$ has a beta-binomial distribution that includes observation error through the estimated crop fraction. A set of seed traps provides a vector of counts $\mathbf{y}_t = y_{1,t}, \dots, y_{n,t}$ that together provide information on tree i through a dispersal kernel. There is conditional independence in fecundity values between trees and within trees over time, taken up by stochastic treatment of $\psi_{i,t}$. There is an additional subscript for location j that is suppressed here to reduce clutter. The full model includes additional elements (see [Model Inference with MASTIF](#)).

245 As in all observational studies, geographic coverage is not uniform. The majority of sites are
 246 temperate (98%), while most observations (tree-years, 80%), trees (58%), and species (74%)
 247 are tropical. Sample sizes are included in Table S1. Sample locations are shown in Fig 2 and
 248 detailed in the Supplement (Figure S1 and Table S1). To assure that results are not dominated
 249 by any one site, we show that the same trends dominate when the largest tropical site, Barro
 250 Colorado Island (BCI), is removed from the analysis (Figure S4).

251 For both CC and ST data types, an observation references a tree-year (a fecundity estimate for
 252 one tree in one year). A crop-count (CC) observation includes the number of fruiting structures
 253 counted (e.g., individual seeds, cones, fruits) and an estimate of the fraction of the total crop

254 represented by the count (see [Model Inference with MASTIF](#)). Where structures bear more than
 255 one seed, numbers are scaled by seeds per structure. For example, *Fagus* capsules bear two
 256 seeds per capsule, and *Pinus* cones bear from 10 to 200 seeds per cone, depending on species.
 257 Seed mass and number of seeds per fruiting structure were taken as an average for the species,
 258 obtained from collections in our labs, supplemented with the TRY Plant Trait Database (Kattge
 259 *et al.*, 2020). A seed-trap (ST) observation includes counts and locations for seed traps on an
 260 inventory plot where each tree is measured and mapped. The uncertainty in a tree-year estimate
 261 depends on the crop-fraction estimate for CC observations and on the redistribution kernel for ST
 262 observations. A beta-binomial distribution for CC data combines uncertainty in the count and
 263 in the crop-fraction estimate. For ST observations, the redistribution model ("dispersal kernel")
 264 quantifies transport to seed traps, a categorical (multinomial) distribution allows for uncertain
 265 seed identification, and a Poisson likelihood allows for variable counts. These data models
 266 link to a common process model for individual fecundity (Figure 3). Stochastic treatment of
 267 fecundity absorbs dependence between observation types, between trees, and within trees over
 268 time. The full model is detailed in Clark *et al.* (2019) and summarized in the section [Model](#)
 269 [Inference with MASTIF](#).

270 Environmental and Individual Covariates

271 Predictors for a given tree-year include diameter, crown class, climate, soil and terrain covariates
 272 (Table S2). Linear and quadratic terms for diameter allow for changes of fecundity with tree
 273 size (Qiu *et al.*, 2021). The crown class assigned to each tree ranges from 1 (full sun) to 5 (full
 274 shade), following the protocol used in the National Ecological Observation Network (NEON)
 275 and the USDA Forest Inventory and Analysis (FIA) program.

276 Climate variables include norms and annual anomalies for temperature (°C) from the previous
 277 year, and moisture surplus (summed monthly precipitation minus evapotranspiration, mm) from
 278 the previous and current years. To allow for changes in moisture access with tree size we
 279 included the interaction between moisture surplus and tree diameter. Climate variables were
 280 derived from [CHELSA](#) (Karger *et al.*, 2017), [TerraClimate](#) (Abatzoglou *et al.*, 2018), and local
 281 climate monitoring data where available. TerraClimate provides monthly but spatially coarse
 282 resolution (Abatzoglou *et al.*, 2018) through 2020. CHELSA provides high spatial resolution (1
 283 km) but CHELSA is not available after 2016. We used regression to project CHELSA climate
 284 forward based on Terraclimate, followed by calibration to local weather data where available.
 285 Details are available in (Clark *et al.*, 2021).

286 Cation exchange capacity (CEC), an indicator of soil fertility (Hazelton & Murphy, 2007),
 287 was obtained from soilGrid250 (Hengl *et al.*, 2017) and used as the weighted mean from three
 288 soil depths: 0-5, 5-15 and 15-30 cm, where weights are the reported uncertainty values. Slope
 289 and aspect were obtained from the global digital elevation model from the NASA shuttle radar
 290 topography mission (Farr *et al.*, 2007) and, for latitudes above 61°, from the USGS National
 291 Elevation Dataset (Gesch *et al.*, 2002). Both products have 30-m resolution. The covariates for
 292 slope and aspect (u_1, u_2, u_3) constitute a length-3 vector,

$$293 \mathbf{u}_j = \begin{cases} u_{j,1} = \sin(s_j) \\ u_{j,2} = \sin(s_j) \sin(a_j) \\ u_{j,3} = \sin(s_j) \cos(a_j) \end{cases} \quad (2)$$

294 for slope s_j , where aspect a_j is taken in radians. These three terms are included as elements of
 295 the design vector $\mathbf{x}_{ij,t}$ (Clark, 1990b).

295 Model Inference with MASTIF

296 The MASTIF model is a (hierarchical) state-space, auto-regressive model that accommodates
 297 dependence between trees and within trees over years through a joint analysis detailed in Clark
 298 *et al.* (2019). For each tree i at location j and year t there is a mean fecundity estimate
 299 $\hat{f}_{ij,t} = \hat{\rho}_{ij,t}\hat{\psi}_{i,t}$ that is the product of conditional fecundity $\hat{\psi}$ and maturation probability $\hat{\rho}_{ij,t}$,
 300 which is the probability that an individual is in the mature state, $z_{ij,t} = 1$. The model for
 301 conditional fecundity is given by $\log \psi_{ij,t} = \mathbf{x}'_{ij,t}\boldsymbol{\beta}^{(x)} + \beta_i^{(w)} + \gamma_{g[i],t} + \epsilon_{i,t}$, where $\mathbf{x}_{ij,t}$ is the
 302 design vector holding climate, soils, local crowding, and individual attributes (Table S2), $\boldsymbol{\beta}^{(x)}$
 303 are fixed-effects coefficients, $\beta_i^{(w)}$ is the random effect for tree i , $\gamma_{g[i],t}$ are year effects that are
 304 random across groups g and fixed for year t , and $\epsilon_{i,t}$ is Gaussian error. To approximate the scale
 305 of potential synchronicity of masting species, the group membership $g[i]$ for tree i is assigned
 306 by species-ecoregion (Clark *et al.*, 2019), using the WWF ecoregion classification (Olson *et al.*,
 307 2001). The principle elements of the model are summarized as a directed acyclic graph (DAG)
 308 in fig. 3.

309 Conditional log fecundity ψ is censored at zero to allow for the immature state and for failed
 310 seed crops in mature individuals,

$$f_{ij,t}|(z_{ij,t} = 1) = \begin{cases} 0 & \psi_{ij,t} \leq 1 \\ \psi_{ij,t} & \psi_{ij,t} > 1 \end{cases} \quad (3)$$

311 This censoring means that seed production requires the potential to produce at least one seed;
 312 the Tobit model uses this censoring to allow for discrete zero observations for otherwise con-
 313 tinuous response variables (Tobin, 1985). For ISP, fecundity is multiplied by mass per seed
 314 and standardized for tree basal area (eq. (1)). For CSP, seed mass is summed over trees on
 315 an inventory plot and divided by plot area. The uncertainty for both quantities is given in the
 316 section [Uncertainty in ISP and CSP](#)

317 The posterior distribution includes parameters and latent variables for maturation state
 318 and tree-year seed production. Posterior simulation uses direct sampling and Metropolis and
 319 Hamiltonian Markov Chain (HMC) updates within Gibbs. Model structure and methodology
 320 was implemented with R (version 4.0, R Core Team 2020) and the R package Mast Inference
 321 and Forecasting (MASTIF), detailed in Clark *et al.* (2019).

322 Uncertainty in ISP and CSP

323 Mean productivity estimates for an individual, ISP, incorporate year-to-year uncertainty for that
 324 tree. Mean productivity estimates for the community, CSP, incorporate tree-to-tree uncertainty
 325 for the inventory plot. We included only trees > 7 cm in diameter, i.e., at least as large as the
 326 smallest measured size in inventory data. Individual fecundity for species s at location j is
 327 evaluated as

$$\hat{f}_{ijs} = \frac{\sum_t w_{ijs,t} \hat{f}_{ijs,t}}{\sum_t w_{ijs,t}} \quad (4)$$

328 where the weight $w_{ijs,t}$ is the inverse of the predictive coefficient of variation for the estimate,
 329 $w_{ijs,t} = CV_{ijs,t}^{-1}$. Th CV is used rather than the predictive standard deviation, because the mean
 330 tends to scale with the variance such that a standard-deviation weight would have the undesirable
 331 property of down-weighting the important large values while up-weighting the less important
 332 low values. ISP combines fecundity from eq. (4) with seed mass and tree basal area in eq. (1).

333 Community seed production is evaluated from the individual means

$$CSP_j = \frac{n_j}{A_j} \frac{\sum_{is} w_{ijs} \hat{f}_{ijs}}{\sum_{is} w_{ijs}} \quad (5)$$

334 where A_j is plot area, n_j is the number of trees, and w_{ijs} is the inverse of the coefficient of
 335 variation given by the root mean predictive variance divided by the predictive mean for tree ij s.
 336 Because CSP requires plot area, only trees on inventory plots are included in the CSP analysis.
 337 Variation in ISP and CSP values were compared across temperature and moisture surplus using
 338 regression.

339 Net Primary Production

340 We extracted Net Primary Production (NPP) from the Moderate Resolution Imaging Spectroradi-
 341 ometry (MODIS) product MOD17 at 500 m resolution (MOD17A3HGFv006, Running *et al.*
 342 2004). We merged yearly CSP estimates with NPP from matching site years, which are available
 343 from 2000 to 2020. Because seed production data span the interval 1959 to 2020, we used the
 344 location-specific mean NPP values for the limited number of earlier years. Because MODIS
 345 NPP is influenced by cloud cover, we compared MODIS NPP values with NPP values from
 346 DGVMs in the S3 experiment of the TRENDY project (Sitch *et al.*, 2015). For each MASTIF
 347 site we averaged NPP from 11 models (CABLE-POP, CLASSIC, CLM5.0, ISAM, JSBACH,
 348 JULES, LPJ-GUESS, LPX, OCN, ORCHIDEE, ORCHIDEE-CNP) and fitted regressions to the
 349 same climate variables used for ISP and CSP (temperature, moisture surplus). The two NPP
 350 products show similar main effects, but differ in the temperature \times moisture interaction, which
 351 is positive for MODIS and negative for the aggregated DGVM. Despite this difference in the
 352 interaction term, main effects dominate the response surfaces that show the same trends for both
 353 NPP sources (Figure S5). Thus, we included only MODIS results in Figure S6.

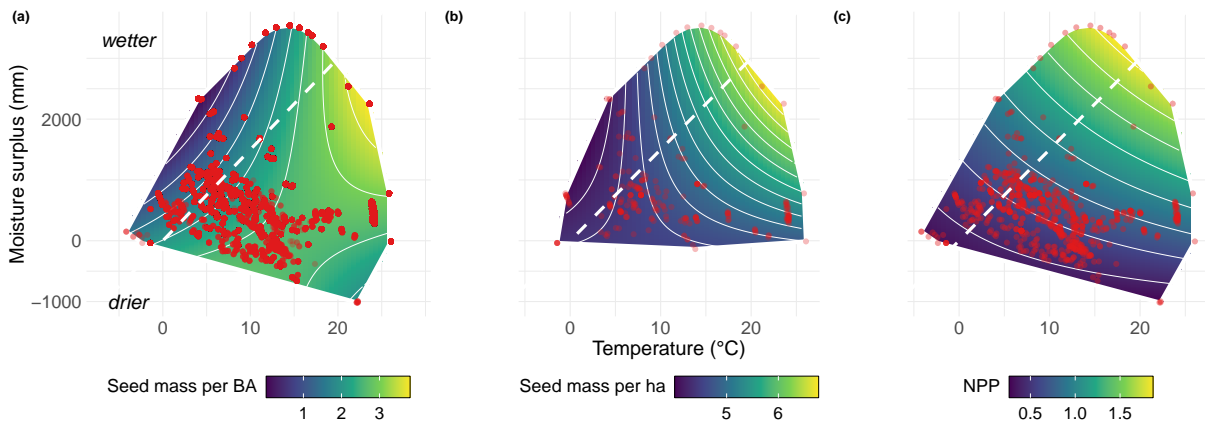


Figure 4: a) Climate responses for (a) ISP (seed production per tree basal area, $\log_{10} \text{ g m}^{-2} \text{ y}^{-1}$) (b) CSP (seed mass per ha forest floor, $\log_{10} \text{ g ha}^{-1} \text{ y}^{-1}$), and (c) NPP ($\text{kg C m}^{-2} \text{ y}^{-1}$). Dashed lines indicate the transect from dry taiga to wet tropics in Fig. 5b. The scales for contours are linear for (c) and \log_{10} for (a) and (b). Convex hulls are defined by observations (red), including individual trees (a, c) and inventory plots (b). Surface predictive standard error are reported in Figure S3. Coefficients are reported in Table S3.

354 Results

355 Community seed production (CSP) increases 250-fold to a global maximum in the warm, moist
 356 tropics, primarily driven by a 100-fold increase in seed production for a given tree size (ISP).

357 ISP and CSP trends with climate align with the geographic trend in NPP (panels in Fig. 4), but
 358 ISP and CSP far exceed the NPP response. The flat ISP (seed production per tree basal area)
 359 response expected if fecundity scales with tree basal area (Fig. 1) contrasts with the observed
 360 100-fold ISP increase along this gradient (Fig. 5), verifying the amplification hypothesized in
 361 Figure 1b. The NPP-scaling assumed in current models (Fig. 1b) is likewise dwarfed by the
 362 CSP rise in seed supply to consumers (Fig. 4b).

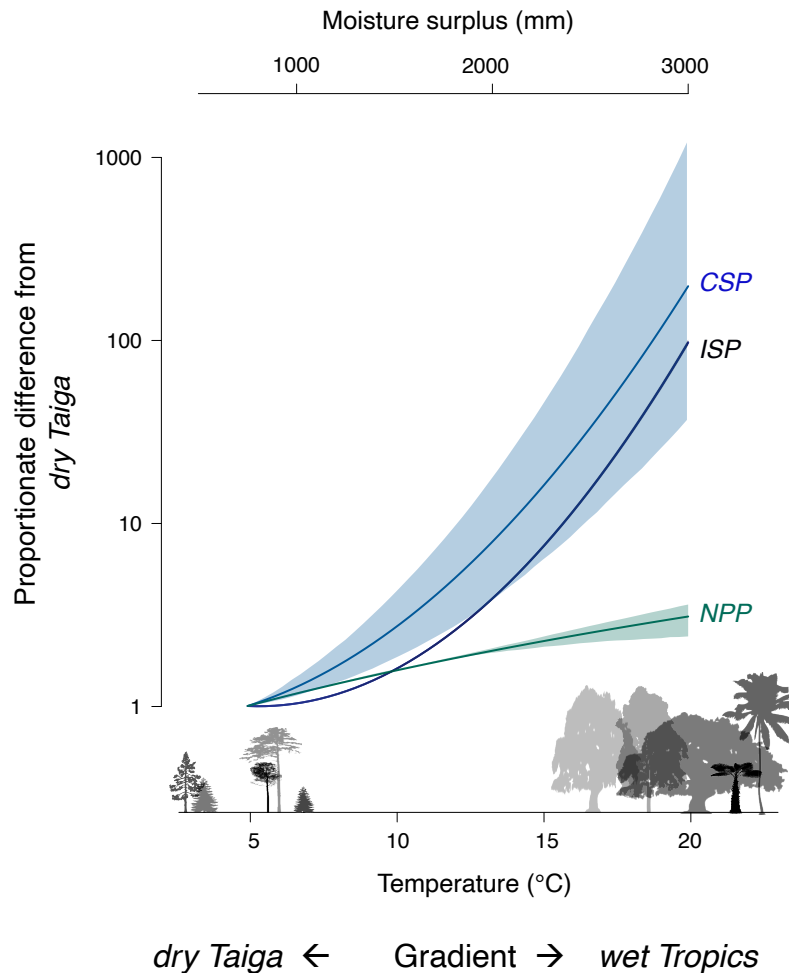


Figure 5: a) Two order of magnitude increases from cold/dry to warm/moist for individual (ISP) and community (CSP) seed production relative to NPP. Curves are sections through surfaces (dashed lines) in Fig. 4, with scales for moisture surplus (above) and temperature (below). Curves are in proportion to values in cold, dry conditions. Confidence intervals (95%) are not visible for ISP and NPP due to the large number of trees. Confidence intervals are wider for CSP due to limited inventory plots at high temperatures (Fig. 2).

363 Despite large trends in ISP and CSP with temperature and moisture (Fig. 5), the latitudinal
 364 contribution to fecundity variation is still lower than contributions of between-tree and the
 365 within-tree (over time) variation (Figure S2). Average seed production for 95% of all trees
 366 of a given size varies over five orders of magnitude, with ISP ranging from 0.000025 to 50
 367 g per cm² of basal area (Figure S7a). Individual variation is matched by that for community
 368 seed production, with 95% of CSP values ranging from 50 g to 2500 kg ha⁻¹ (Figure S7b).
 369 Tree-to-tree variation combines for an increase in ISP to highest values in warm, moist climates
 370 (Fig. 4a, b) that is driven more by temperature than by moisture (Table S3); the temperature
 371 response is amplified by moisture where temperatures are high (Figure S2c). The fact that the

372 massive geographic trend in Fig. 5 can be masked by tree-to-tree and year-to-year variation
 373 (these sources are partitioned in Clark *et al.* 2004) emphasizes the importance of large data sets
 374 that span broad coverage in individual condition, habitat, and climate (Qiu *et al.*, 2021).

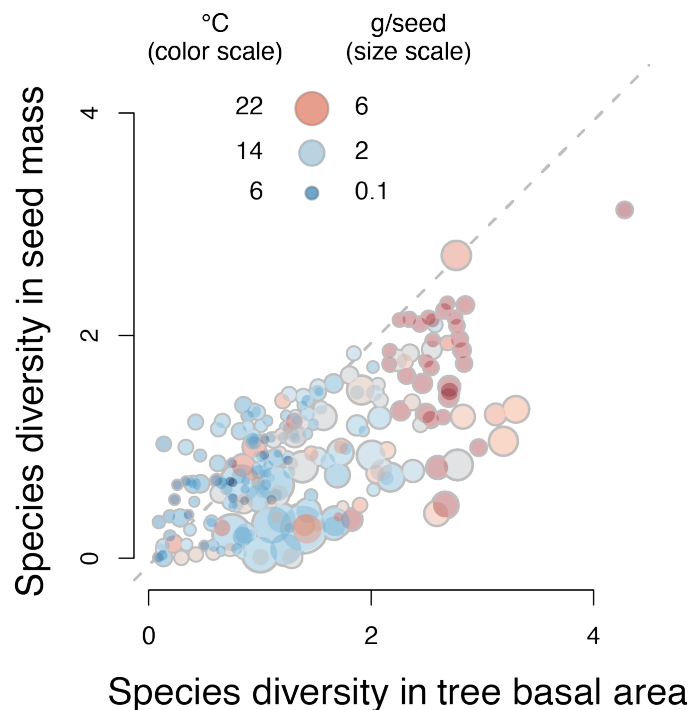


Figure 6: Species diversity in seeds (vertical axis) is lower than expected from species diversity in trees (horizontal axis). In both cases, diversity is evaluated from the Shannon index, $-\sum_s p_s \log p_s$, where p_s is the fraction of species s in basal area (trees) and CSP (seed mass). Each point represents an inventory plot. Except at low tree diversity, points lie almost entirely below the 1:1 line (dashed). The legend at top left shows mean annual temperature (symbol color) and mass of the average seed (symbol size).

375 Forest productivity does not explain the global fecundity gradient evident at the individual
 376 and community levels. The parallel 100- and 250-fold increases for ISP and CSP (Fig. 5b) to
 377 maxima in warm, moist climates (Fig. 4) spans only a three-fold range for NPP. The trends in
 378 both ISP and CSP mean that not only do individual trees produce more seed for a given size
 379 in the wet tropics, but also that seed abundance is amplified at the community level (Figure 4a,
 380 b). [Community-level CSP need not necessarily track ISP responses due to heterogeneous
 381 size-species structures associated with local site conditions, past disturbance, and competition].

382 Discussion

383 The 250-fold latitudinal trend in tree seed production exceeds expectations from previous studies.
 384 The possibility that seed production might be highest at low latitudes and that seed production
 385 might not be explained by productivity was suggested from mean counts in 18 forest seed-trap
 386 studies (Moles *et al.*, 2009). New estimates reported here reflect an extension to large sample
 387 sizes, direct inference on seed production by each tree (rather than counts within traps), and use
 388 of seed mass for the species (rather than a mean value across all species at the same latitude).
 389 With synthetic modeling of 12M observations on 753 species we extend the previous discovery
 390 of a fecundity hotspot in the warm, moist southeastern North America (Clark *et al.*, 2021) to a
 391 global phenomenon.

392 Biogeographic trends reported here complement studies that focus on interannual varia-
393 tion, or "masting". Temporal variation in climate (Clark *et al.*, 2014; Caignard *et al.*, 2017;
394 Bogdziewicz *et al.*, 2020a) are of great interest for understanding allocation shifts within indi-
395 viduals over time (Koenig, 2021), but these interactions fundamentally differ from geographic
396 variation in populations subjected to divergent selection histories (Clark *et al.*, 2014). Results
397 here provide a geographic context for variation within species and communities and the variables
398 that control variation.

399 Improving forest regeneration in DGVMs might shift from the current focus on sharpening
400 estimates of reproduction as a fraction of NPP (Fisher *et al.*, 2018; Hanbury-Brown *et al.*, 2022)
401 to a recognition of how fecundity responses diverge from NPP. Results from figure 5 show that
402 the DGVM assumption of fecundity as a simple fraction of NPP misses the key controls at stand
403 and regional scales. Clearly, reproduction is not a residual sink to be filled after growth and
404 other demands are satisfied. Previous understanding shows the assumption of reproduction as a
405 constant fraction of NPP to be unrealistic at the individual scale (fecundity is far more volatile
406 than annual resource capture or growth) (Clark *et al.*, 2004; Sala *et al.*, 2012; Clark *et al.*, 2014;
407 Berdanier & Clark, 2016). The climate trends in Figure 5 show that NPP scaling also does not
408 work as a community-level summary. Fecundity responses to local habitat and regional climate
409 reported here can enter models directly.

410 Amplified fecundity in warm, moist climates, beyond what could be explained by trends in
411 NPP (Fig. 5), may represent a direct climate response or the legacy of adaptive evolution to
412 intense species interactions. By quantifying both individual and community seed productivity
413 (ISP, CSP), we show that the community response is driven primarily by the fact that trees of
414 a given size produce, on average, 100 times the seed mass in the wet tropics. This latitudinal
415 trend in ISP is then amplified to a 250-fold trend in CSP (seed production per area) by the
416 greater abundances of large trees in the wet tropics. Amplification beyond the trend in NPP may
417 result from flexibility in seed production to respond to a longer growing season (Yeoh *et al.*,
418 2017; Mendoza *et al.*, 2018) well in excess of tree growth, which is limited by mechanical and
419 hydraulic constraints on tree size (Koch *et al.*, 2004; King *et al.*, 2009). At the community scale,
420 NPP is further constrained by the compensatory losses in stand biomass as mortality increases
421 to offset increases in growth (Assmann, 1970; Clark, 1990a). Thus, while NPP increases with
422 warm, wet conditions, the lack of structural constraints on producing more seeds might allow
423 for a disproportionate fecundity response in Figure 1. Alternatively, amplification could also
424 be driven by intense species interactions that select for reproduction to offset high losses to
425 consumers and enhance the benefits of frugivory (Terborgh, 1986; Harms *et al.*, 2000; Hille
426 Ris Lambers *et al.*, 2002; Schemske *et al.*, 2009; Levi *et al.*, 2019; Hargreaves *et al.*, 2019).

427 Whether amplification occurs as a direct response to climate or as an adaptive response to in-
428 tense biotic interactions, the density- and frequency-dependent processes involving competition,
429 consumers, and seed dispersers have community-wide implications. The two order-of-magnitude
430 climatic and latitudinal trend in seed mass per forest-floor area (CSP) has direct implications for
431 density-dependent interactions, which include competition within tree species and frequency-
432 dependent consumers. Elevated seed supply and the offsetting mortality losses affect selective
433 pressure for competitive phenotypes. The bottom-up enrichment of food webs that cascades to
434 higher trophic levels (Ostfeld & Keesing, 2000; Rosenblatt & Schmitz, 2016; Levi *et al.*, 2019)
435 can increase consumer and disperser densities that, in turn, impose frequency-dependence se-
436 lection on seed and seedling survival (Janzen, 1970). The magnitude of amplification suggests
437 that seed supply intensifies species interactions in the wet tropics.

438 Frequency-dependent consumer pressures depend on diversity of the seed resource, which
439 is poorly predicted by the standard inventory of trees. Using Shannon entropy $[-\sum_s p_s \log p_s$,

440 where p_s is the fraction of species s in basal area (trees) and CSP (seed mass)], species diversity
441 of both seed productivity and tree basal area is highest in the warm tropics. However, tree
442 diversity exceeds the diversity of the seed resource in warm climates (Fig. 6). The lower species
443 diversity for seeds than for trees in warm climates results from the fact that species having
444 modest differences in tree basal area vary widely in fecundity; tendency for a subset of species
445 to dominate seed production reduces seed diversity below that for trees. Conversely, in the cool
446 climates where seeds tend to be small (small, blue symbols in Fig. 6), the low diversity that would
447 be estimated on the basis of trees can mask an unexpectedly high seed diversity. Although many
448 studies do not record fecundity for species having the smallest seeds (e.g., Salicaceae), these
449 are also the seeds that are least apparent to many consumers. Omission of these smallest seeds
450 from this study means that values of seed production are under-estimates, but still relevant for
451 many consumers. The net effect of overestimating seed diversity in warm climates is important
452 for frequency-dependent processes (Green *et al.*, 2014), such as host-specific seed predation.

453 Whether the 100-fold biogeographic gradient is driven by biophysical constraints on alloca-
454 tion or adaptive evolution to differing consumer pressures, these results add a new dimension
455 to the understanding of trophic processes that may control latitudinal diversity gradients. If
456 host-specific consumers regulate diversity through density- and frequency-dependent attack,
457 then the strongest impacts are occurring where seed supply can support the highest numbers of
458 consumers. Through shared consumers and frugivores, fecundity of many species can contribute
459 to the selection pressures on competitors and consumers (Whitham *et al.*, 2020; Bogdziewicz
460 *et al.*, 2020b). The dramatic biogeographic trend in seed supply sets up the potential for an
461 evolutionary arms race (Dawkins & Krebs, 1979; Gruntman *et al.*, 2017) as selective pres-
462 sures balance the benefits of producing more seed against the full costs of increased fecundity
463 (Obeso, 2002; Pincheira-Donoso & Hunt, 2015; Fridley, 2017), including diverting resources
464 from growth and defense (Berdanier & Clark, 2016; Lauder *et al.*, 2019). A positive feedback
465 on selection pressure in diverse tropical forests could ensue where species from every major
466 angiosperm clade enrich functional space and niche overlap. Regardless of whether this arms
467 race has occurred, the trends in stand-level seed rain have profound implications for food web
468 dynamics.

469 Our results show that climate change impact on tree fecundity will not scale simply with
470 change in productivity. Climate change induced changes in seed production will come with feed-
471 backs through shared consumers and dispersers (Bogdziewicz *et al.*, 2020b). The temperature-
472 tropical gradient in seed production reported here could motivate research on climate effect on
473 seed production, their consumers and dispersers (Hargreaves *et al.*, 2019).

References

- 474
- 475 Abatzoglou, J.T., Dobrowski, S.Z., Parks, S.A. & Hegewisch, K.C. (2018). Terraclimate, a high-
476 resolution global dataset of monthly climate and climatic water balance from 1958–2015.
477 *Scientific Data*, 5, 170191.
- 478 Assmann, E. (1970). *The principles of forest yield study. Studies in the organic production,*
479 *structure, increment and yield of forest stands.*
- 480 Berdanier, A.B. & Clark, J.S. (2016). Divergent reproductive allocation trade-offs with canopy
481 exposure across tree species in temperate forests. *Ecosphere*, 7, e01313–n/a.
- 482 Bogdziewicz, M., Fernández-Martínez, M., Espelta, J.M., Ogaya, R. & Penuelas, J. (2020a). Is
483 forest fecundity resistant to drought? Results from an 18-yr rainfall-reduction experiment.
484 *New Phytologist*, 227, 1073–1080.
- 485 Bogdziewicz, M., Kelly, D., Thomas, P.A., Lageard, J.G. & Hacket-Pain, A. (2020b). Climate
486 warming disrupts mast seeding and its fitness benefits in European beech. *Nature Plants*, 6,
487 88–94.
- 488 Brienen, R.J., Caldwell, L., Duchesne, L., Voelker, S., Barichivich, J., Baliva, M. *et al.* (2020).
489 Forest carbon sink neutralized by pervasive growth-lifespan trade-offs. *Nature Communica-*
490 *tions*, 11, 1–10.
- 491 Caignard, T., Kremer, A., Firmat, C., Nicolas, M., Venner, S. & Delzon, S. (2017). Increasing
492 Spring Temperatures Favor Oak Seed Production in Temperate Areas. *Scientific Reports*, 7,
493 1–8.
- 494 Chu, C., Lutz, J.A., Král, K., Vrška, T., Yin, X., Myers, J.A. *et al.* (2019). Direct and indirect
495 effects of climate on richness drive the latitudinal diversity gradient in forest trees. *Ecology*
496 *Letters*, 22, 245–255.
- 497 Clark, J.S. (1990a). Integration of ecological levels: Individual plant growth, population
498 mortality and ecosystem processes. *Journal of Ecology*, 78, 275–299.
- 499 Clark, J.S. (1990b). Landscape interactions among nitrogen mineralization, species composition,
500 and long-term fire frequency. *Biogeochemistry*, 11, 1–22.
- 501 Clark, J.S., Andrus, R., Aubry-Kientz, M., Bergeron, Y., Bogdziewicz, M., Bragg, D.C. *et al.*
502 (2021). Continent-wide tree fecundity driven by indirect climate effects. *Nature Communi-*
503 *cations*, 12, 1–11.
- 504 Clark, J.S., Bell, D.M., Kwit, M.C. & Zhu, K. (2014). Competition-interaction landscapes for
505 the joint response of forests to climate change. *Global Change Biology*, 20, 1979–1991.
- 506 Clark, J.S., LaDeau, S. & Ibanez, I. (2004). Fecundity of trees and the colonization-competition
507 hypothesis. *Ecological Monographs*, 74, 415–442.
- 508 Clark, J.S., Nuñez, C.L. & Tomasek, B. (2019). Foodwebs based on unreliable foundations:
509 spatiotemporal masting merged with consumer movement, storage, and diet. *Ecological*
510 *Monographs*, 89, 1–24.

- 511 Corlett, R.T. (2013). The shifted baseline: Prehistoric defaunation in the tropics and its conse-
512 quences for biodiversity conservation. *Biological Conservation*, 163, 13–21.
- 513 Dawkins, R. & Krebs, J.R. (1979). Arms races between and within species. *Proceedings of the*
514 *Royal Society of London. Series B, Biological Sciences*, 205, 489–511.
- 515 Del Grosso, S., Parton, W., Stohlgren, T., Zheng, D., Bachelet, D., Prince, S. *et al.* (2008).
516 Global Potential Net Primary Production Predicted from Vegetation Class, Precipitation, and
517 Temperature. *Ecology*, 89, 2117–2126.
- 518 Farr, T.G., Rosen, P.A., Caro, E., Crippen, R., Duren, R., Hensley, S. *et al.* (2007). The shuttle
519 radar topography mission. *Reviews of Geophysics*, 45.
- 520 Fisher, R.A., Koven, C.D., Anderegg, W.R., Christoffersen, B.O., Dietze, M.C., Farrior, C.E.
521 *et al.* (2018). Vegetation demographics in Earth System Models: A review of progress and
522 priorities. *Global Change Biology*, 24, 35–54.
- 523 Fridley, J.D. (2017). Plant energetics and the synthesis of population and ecosystem ecology.
524 *Journal of Ecology*, 105, 95–110.
- 525 Gesch, D., Oimoen, M., Greenlee, S., Nelson, C., Steuck, M. & Tyler, D. (2002). The National
526 Elevation Dataset. In: *Photogrammetric Engineering and Remote Sensing*. American Society
527 for Photogrammetry and Remote Sensing, vol. 68, pp. 5–11.
- 528 Green, P.T., Harms, K.E. & Connell, J.H. (2014). Nonrandom, diversifying processes are
529 disproportionately strong in the smallest size classes of a tropical forest. *Proceedings of the*
530 *National Academy of Sciences*, 111, 18649–18654.
- 531 Gruntman, M., Groß, D., Májeková, M. & Tielbörger, K. (2017). Decision-making in plants
532 under competition. *Nature Communications*, 8, 2235.
- 533 Hanbury-Brown, A., Ward, R. & Kueppers, L.M. (2022). Future forests within earth system
534 models: regeneration processes critical to prediction. *New Phytologist*, in press, 000–000.
- 535 Hargreaves, A.L., Suárez, E., Mehltreter, K., Myers-Smith, I., Vanderplank, S.E., Slinn, H.L.
536 *et al.* (2019). Seed predation increases from the Arctic to the Equator and from high to low
537 elevations. *Science Advances*, 5, 1–11.
- 538 Harms, K.E., Wright, S.J., Calderón, O., Hernández, A. & Herre, E.A. (2000). Pervasive
539 density-dependent recruitment enhances seedling diversity in a tropical forest. *Nature*, 404,
540 493–495.
- 541 Hazelton, P. & Murphy, B. (2007). *Interpreting soil test results: What do all the numbers mean?*
542 CSIRO publishing.
- 543 Hengl, T., De Jesus, J.M., Heuvelink, G.B., Gonzalez, M.R., Kilibarda, M., Blagotić, A. *et al.*
544 (2017). SoilGrids250m: Global gridded soil information based on machine learning. *PLoS*
545 *ONE*, 12.
- 546 Hille Ris Lambers, J., Clark, J.S. & Beckage, B. (2002). Density-dependent mortality and the
547 latitudinal gradient in species diversity. *Nature*, 417, 732–735.
- 548 Janzen, D. (1970). Herbivores and the number of tree species in tropical forests. *The American*
549 *Naturalist*, 104, 501–528.

- 550 Karger, D.N., Conrad, O., Böhner, J., Kawohl, T., Kreft, H., Soria-Auza, R.W. *et al.* (2017).
551 Climatologies at high resolution for the earth's land surface areas. *Scientific Data*, 4, 1–20.
- 552 Kattge, J., Bönisch, G., Díaz, S., Lavorel, S., Prentice, I.C., Leadley, P. *et al.* (2020). TRY plant
553 trait database – enhanced coverage and open access. *Global Change Biology*, 26, 119–188.
- 554 King, D.A., Davies, S.J., Tan, S. & Md. Noor, N.S. (2009). Trees approach gravitational limits
555 to height in tall lowland forests of malaysia. *Functional Ecology*, 23, 284–291.
- 556 Koch, G.W., Sillett, S.C., Jennings, G.M. & Davis, S.D. (2004). The limits to tree height.
557 *Nature*, 428, 851–854.
- 558 Koenig, W.D. (2021). A brief history of masting research. *Philosophical Transactions of the*
559 *Royal Society B: Biological Sciences*, 376, 20200423.
- 560 Krinner, G., Viovy, N., de Noblet-Ducoudré, N., Ogée, J., Polcher, J., Friedlingstein, P. *et al.*
561 (2005). A dynamic global vegetation model for studies of the coupled atmosphere-biosphere
562 system. *Global Biogeochemical Cycles*, 19, 1–33.
- 563 LaMontagne, J.M., Pearse, I.S., Greene, D.F. & Koenig, W.D. (2020). Mast seeding patterns
564 are asynchronous at a continental scale. *Nature Plants*, 6, 460–465.
- 565 Lauder, J.D., Moran, E.V. & Hart, S.C. (2019). Fight or flight? potential tradeoffs between
566 drought defense and reproduction in conifers. *Tree Physiology*, 39, 1071–1085.
- 567 Levi, T., Barfield, M., Barrantes, S., Sullivan, C., Holt, R.D. & Terborgh, J. (2019). Tropical
568 forests can maintain hyperdiversity because of enemies. *Proceedings of the National Academy*
569 *of Sciences*, 116, 581–586.
- 570 Lewis, S.L., Phillips, O.L., Sheil, D., Vinceti, B., Baker, T.R., Brown, S. *et al.* (2004). Tropical
571 forest tree mortality, recruitment and turnover rates: Calculation, interpretation and compar-
572 ison when census intervals vary. *Journal of Ecology*, 92, 929–944.
- 573 Locosselli, G.M., Brienen, R.J.W., Leite, M.d.S., Gloor, M., Krottenthaler, S., Oliveira, A.A.d.
574 *et al.* (2020). Global tree-ring analysis reveals rapid decrease in tropical tree longevity with
575 temperature. *Proceedings of the National Academy of Sciences*, 117, 33358–33364.
- 576 Mendoza, I., Condit, R.S., Wright, S.J., Caubère, A., Châtelet, P., Hardy, I. *et al.* (2018). Inter-
577 annual variability of fruit timing and quantity at Nouragues (French Guiana): insights from
578 hierarchical Bayesian analyses. *Biotropica*, 50, 431–441.
- 579 Minor, D.M. & Kobe, R.K. (2019). Fruit production is influenced by tree size and size-
580 asymmetric crowding in a wet tropical forest. *Ecology and Evolution*, 9, 1458–1472.
- 581 Mokany, K., Prasad, S. & Westcott, D.A. (2014). Loss of frugivore seed dispersal services under
582 climate change. *Nature Communications*, 5, 3971.
- 583 Moles, A.T., Wright, I.J., Pitman, A.J., Murray, B.R. & Westoby, M. (2009). Is there a latitudinal
584 gradient in seed production? *Ecography*, 32, 78–82.
- 585 Obeso, J.R. (2002). The costs of reproduction in plants. *New Phytologist*, 155, 321–348.

- 586 Olson, D.M., Dinerstein, E., Wikramanayake, E.D., Burgess, N.D., Powell, G.V., Underwood,
587 E.C. *et al.* (2001). Terrestrial ecoregions of the world: A new map of life on Earth. *BioScience*,
588 51, 933–938.
- 589 Ostfeld, R.S. & Keesing, F. (2000). Pulsed resources and community dynamics of consumers
590 in terrestrial ecosystems. *Trends in Ecology and Evolution*, 15, 232–237.
- 591 Pearse, I.S., LaMontagne, J.M., Lordon, M., Hipp, A.L. & Koenig, W.D. (2020). Biogeography
592 and phylogeny of masting: do global patterns fit functional hypotheses? *New Phytologist*,
593 227, 1557–1567.
- 594 Phillips, O.L. & Gentry, A.H. (1994). Increasing turnover through time in tropical forests.
595 *Science*, 263, 954–958.
- 596 Pincheira-Donoso, D. & Hunt, J. (2015). Fecundity selection theory: Concepts and evidence.
597 *Biological reviews of the Cambridge Philosophical Society*, 92.
- 598 Qiu, T., Aravena, M.C., Andrus, R., Ascoli, D., Bergeron, Y., Berretti, R. *et al.* (2021). Is there
599 tree senescence? The fecundity evidence. *Proceedings of the National Academy of Sciences*
600 *of the United States of America*, 118, 1–10.
- 601 R Core Team (2020). *R: A Language and Environment for Statistical Computing*. R Foundation
602 for Statistical Computing, Vienna, Austria.
- 603 Rosenblatt, A.E. & Schmitz, O.J. (2016). Climate change, nutrition, and bottom-up and top-
604 down food web processes. *Trends in Ecology and Evolution*, 31, 965–975.
- 605 Running, S.W., Nemani, R.R., Heinsch, F.A., Zhao, M., Reeves, M. & Hashimoto, H. (2004).
606 A continuous satellite-derived measure of global terrestrial primary production. *BioScience*,
607 54, 547–560.
- 608 Sala, A., Hopping, K., McIntire, E.J.B., Delzon, S. & Crone, E.E. (2012). Masting in whitebark
609 pine (*Pinus albicaulis*) depletes stored nutrients. *New Phytologist*, 196, 189–199.
- 610 Schemske, D.W., Mittelbach, G.G., Cornell, H.V., Sobel, J.M. & Roy, K. (2009). Is there a
611 latitudinal gradient in the importance of biotic interactions? *Annual Review of Ecology,*
612 *Evolution, and Systematics*, 40, 245–269.
- 613 Sharma, S., Bergeron, Y., Bogdziewicz, M., Bragg, D., Brockway, D., Cleavitt, N. *et al.*
614 (2021). North American tree migration paced by recruitment through contrasting east-west
615 mechanisms. *Proceedings of the National Academy of Sciences*, in press.
- 616 Sitch, S., Friedlingstein, P., Gruber, N., Jones, S.D., Murray-Tortarolo, G., Ahlström, A. *et al.*
617 (2015). Recent trends and drivers of regional sources and sinks of carbon dioxide. *Biogeo-*
618 *sciences*, 12, 653–679.
- 619 Sitch, S., Smith, B., Prentice, I.C., Arneth, A., Bondeau, A., Cramer, W. *et al.* (2003). Evaluation
620 of ecosystem dynamics, plant geography and terrestrial carbon cycling in the LPJ dynamic
621 global vegetation model. *Global Change Biology*, 9, 161–185.
- 622 Stephenson, N.L. & Van Mantgem, P.J. (2005). Forest turnover rates follow global and regional
623 patterns of productivity. *Ecology Letters*, 8, 524–531.

- 624 Terborgh, J. (1986). *Community aspects of frugivory in tropical forests*, Springer, Dordrecht,
625 vol. 15 of *Tasks for Vegetation Science*.
- 626 Tobin, B.Y.J. (1985). Estimation of Relationships for Limited Dependent Variables. *Economet-*
627 *rica*, 26, 24–36.
- 628 Vacchiano, G., Ascoli, D., Berzaghi, F., Lucas-Borja, M.E., Caignard, T., Collalti, A. *et al.*
629 (2018). Reproducing reproduction: How to simulate mast seeding in forest models. *Ecological*
630 *Modelling*, 376, 40–53.
- 631 Westoby, M., Jurado, E. & Leishman, M. (1992). Comparative evolutionary ecology of seed
632 size. *Trends in Ecology and Evolution*, 7, 368–372.
- 633 Whitham, T.G., Allan, G.J., Cooper, H.F. & Shuster, S.M. (2020). Intraspecific genetic variation
634 and species interactions contribute to community evolution. *Annual Review of Ecology,*
635 *Evolution, and Systematics*, 51, 587–612.
- 636 Yeoh, S.H., Satake, A., Numata, S., Ichie, T., Lee, S.L., Basherudin, N. *et al.* (2017). Unrav-
637 elling proximate cues of mass flowering in the tropical forests of South-East Asia from gene
638 expression analyses. *Molecular Ecology*, 26, 5074–5085.

639 **Acknowledgements**

640 We thank the National Ecological Observatory Network (NEON) for access to sites and veg-
641 etation structure data, W. Koenig and F. Lefèvre for additional data, and S. Sitch for access
642 to TRENDY products. The project has been funded by grants to JSC from the National Sci-
643 ence Foundation, most recently DEB-1754443, and by the Belmont Forum (1854976), NASA
644 (AIST16-0052, AIST18-0063), and the Programme d'Investissement d'Avenir under project
645 FORBIC (18-MPGA-0004) (*Make Our Planet Great Again*). Jerry Franklin's data remain ac-
646 cessible through NSF LTER DEB-1440409. Puerto Rico data were funded by NSF grants,
647 most recently, DEB 0963447 and LTREB 11222325. Data from the Andes Biodiversity and
648 Ecosystem Research Group were funded by the Gordon and Betty Moore Foundation and NSF
649 LTREB 1754647. MB was supported by grant no. 2019/35/D/NZ8/00050 from the (Polish) Na-
650 tional Science Centre, and Polish National Agency for Academic Exchange Bekker programme
651 PPN/BEK/2020/1/00009/U/00001. Research by the USDA Forest Service and the the USGS
652 was funded by these agencies. Any use of trade, firm, or product names does not imply endorse-
653 ment by the U.S. Government.

654

655 **Competing interests**

656 The authors declare no competing interests

657

658 **Supporting Information**

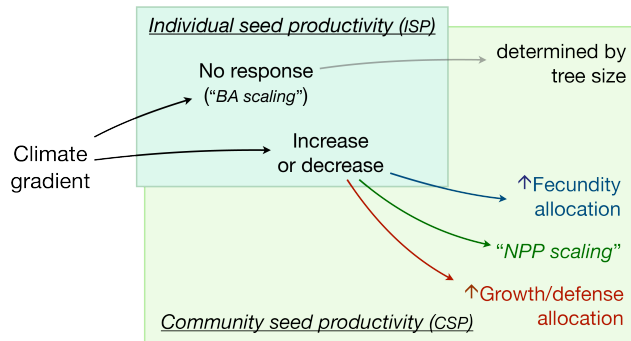
659 Table S1 – S3

660 Fig S1 - S7

661 **List of Figures**

662 **Figures**

a) Individual and community response



b) CSP and NPP responses

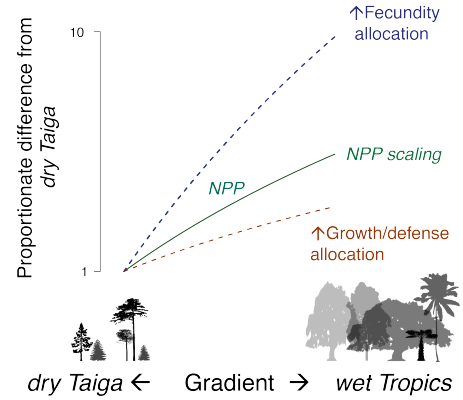


Figure 1: a) Individual seed productivity (ISP, seed mass per tree basal area) might not vary with latitudinal climate gradients, in which case community seed productivity (CSP, seed mass production per forest area) depends on variation in tree size. Alternatively, responses could depend on net primary productivity (NPP), increasing if allocation in warm climates shifts preferentially to fecundity or decreasing if allocation in warm climates shifts to growth and defenses. b) Proportionate differences in fecundity hypothesized for the three scenarios in (a) shown as differences from the climate gradient in NPP. The NPP-scaling scenario means that NPP and CSP follow the same proportionate trajectory (green line).

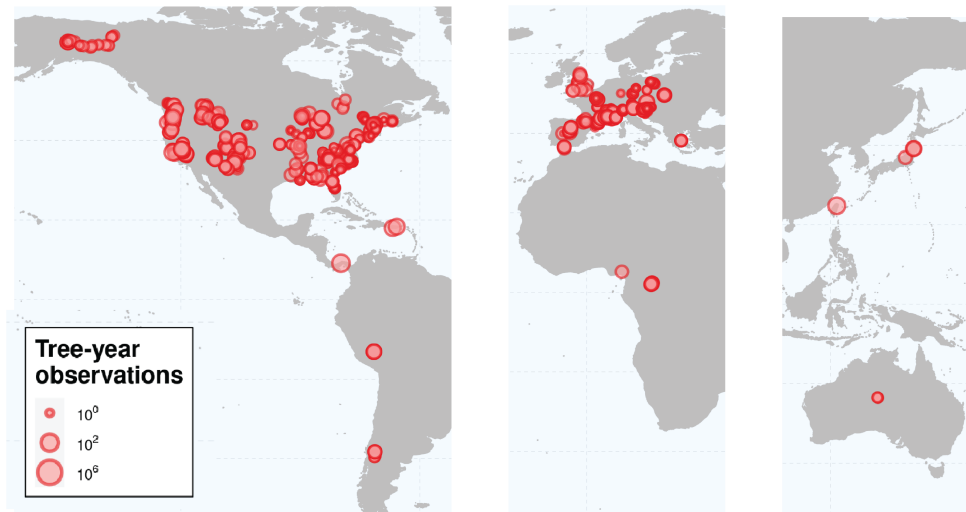


Figure 2: MASTIF data summary, with symbol size proportional to observations. The distribution of data is detailed in Figure S1 and in Table S1.

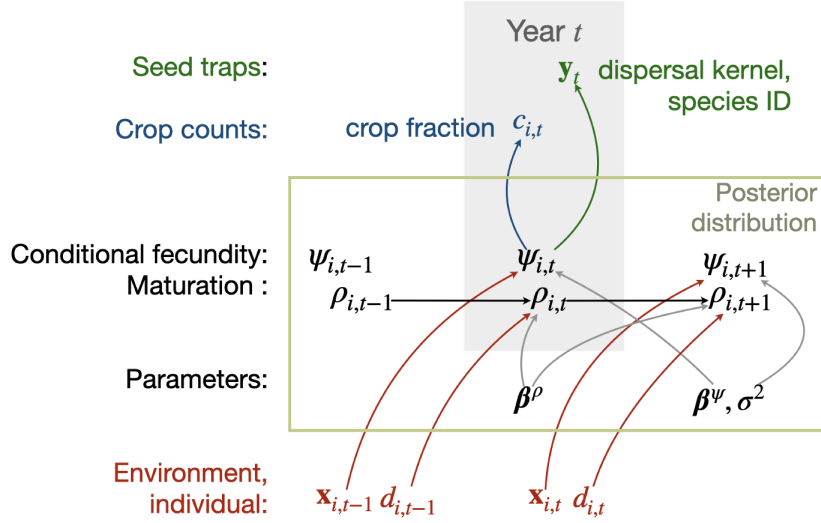


Figure 3: The MASTIF model simplified from Clark *et al.* (2019) to emphasize variables and parameters discussed in the text. A biophysical model for change in fecundity $\psi_{i,t}$ of tree i in year t (a tree-year) is driven by individual tree condition and climate and habitat variables in design vector $\mathbf{x}_{i,t}$ with corresponding coefficients β . Maturation status incorporates tree diameter $d_{i,t}$. The hierarchical state-space model includes process error variance σ^2 and observation error in two data types. A crop count $c_{i,t}$ has a beta-binomial distribution that includes observation error through the estimated crop fraction. A set of seed traps provides a vector of counts $\mathbf{y}_t = y_{1,t}, \dots, y_{n,t}$ that together provide information on tree i through a dispersal kernel. There is conditional independence in fecundity values between trees and within trees over time, taken up by stochastic treatment of $\psi_{i,t}$. There is an additional subscript for location j that is suppressed here to reduce clutter. The full model includes additional elements (see [Model Inference with MASTIF](#)).

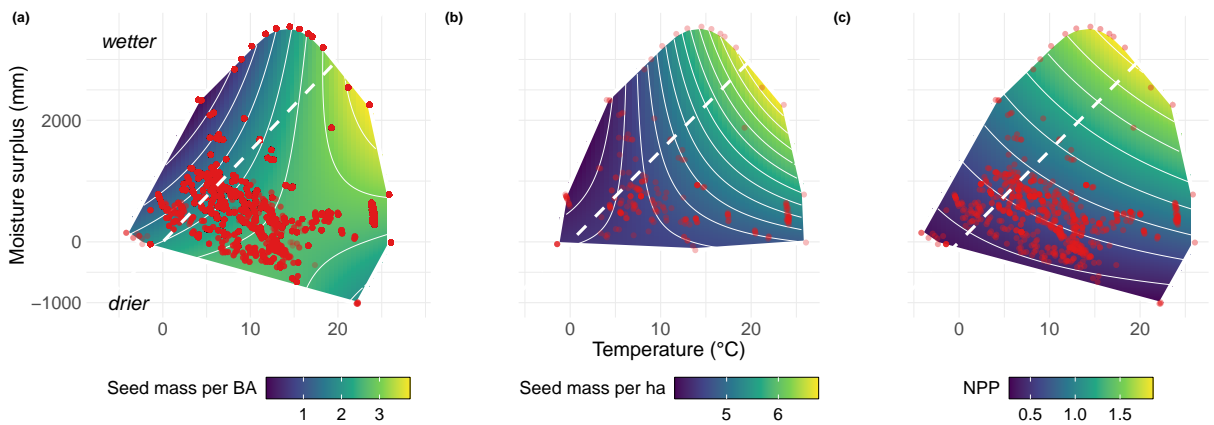


Figure 4: a) Climate responses for (a) ISP (seed production per tree basal area, $\log_{10} \text{ g m}^{-2} \text{ y}^{-1}$) (b) CSP (seed mass per ha forest floor, $\log_{10} \text{ g ha}^{-1} \text{ y}^{-1}$), and (c) NPP ($\text{kg C m}^{-2} \text{ y}^{-1}$). Dashed lines indicate the transect from dry taiga to wet tropics in Fig. 5b. The scales for contours are linear for (c) and \log_{10} for (a) and (b). Convex hulls are defined by observations (red), including individual trees (a, c) and inventory plots (b). Surface predictive standard error are reported in Figure S3. Coefficients are reported in Table S3.

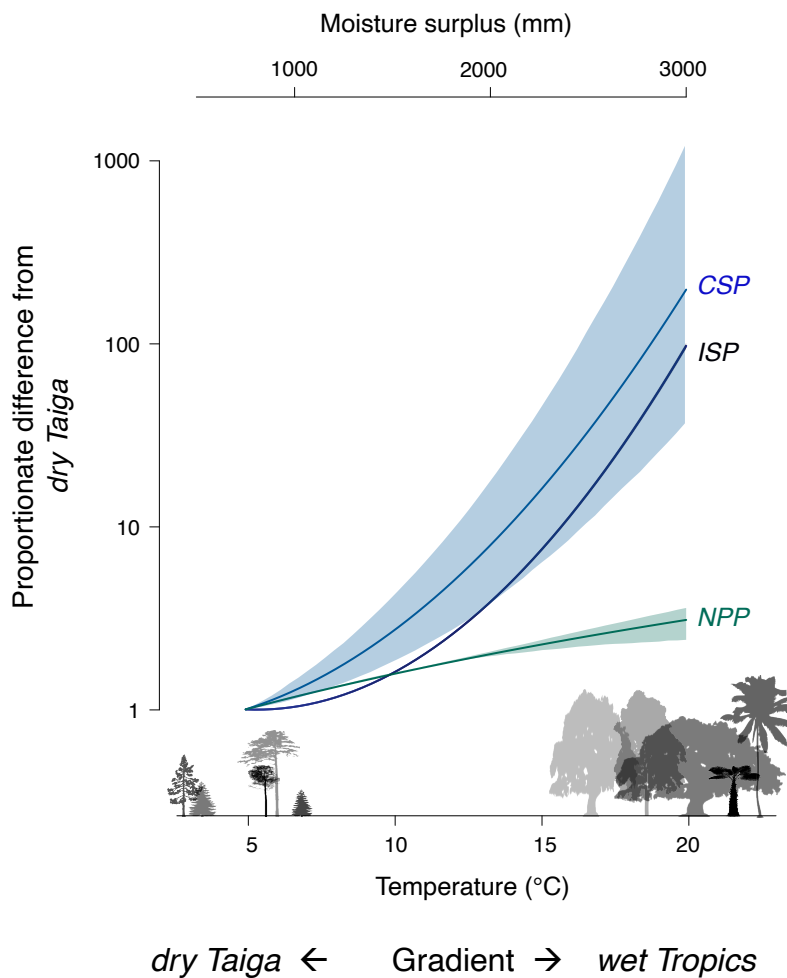


Figure 5: a) Two order of magnitude increases from cold/dry to warm/moist for individual (ISP) and community (CSP) seed production relative to NPP. Curves are sections through surfaces (dashed lines) in Fig. 4, with scales for moisture surplus (above) and temperature (below). Curves are in proportion to values in cold, dry conditions. Confidence intervals (95%) are not visible for ISP and NPP due to the large number of trees. Confidence intervals are wider for CSP due to limited inventory plots at high temperatures (Fig. 2).

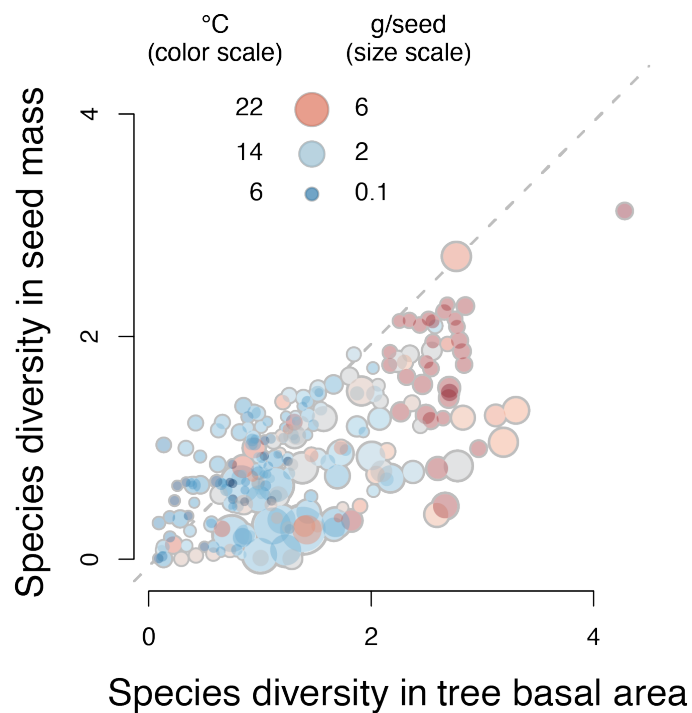


Figure 6: Species diversity in seeds (vertical axis) is lower than expected from species diversity in trees (horizontal axis). In both cases, diversity is evaluated from the Shannon index, $-\sum_s p_s \log p_s$, where p_s is the fraction of species s in basal area (trees) and CSP (seed mass). Each point represents an inventory plot. Except at low tree diversity, points lie almost entirely below the 1:1 line (dashed). The legend at top left shows mean annual temperature (symbol color) and mass of the average seed (symbol size).

663 Supporting Information

664 Globally, tree fecundity exceeds productivity gradients

665 Valentin Journé *et al.*, Ecology Letters

666

667 This Supplement provides additional data summaries as tables and figures. Full summaries of
668 the [MASTIF network](#) are available these links for [sites](#) and [species](#).

669 Supplementary Tables

Table S1: Numbers of species, stands, trees, and tree-years for ISP analysis and complete inventories for CSP analysis by tropical and temperate regions. Complete inventories include all trees within a mapped plot and are needed to determine seeds per area in CSP. Because not all inventory plots use the same minimum diameter, the latter is based on trees > 7 cm.

Floristic Region	Species	Sites	Tree-years	Trees	Complete inventories
Tropical	559	64	9,723,438	85,261	47
Temperate	194	3506	2,330,294	61,461	204

Table S2: Covariates used to fit the MASTIF model and data sources. Subscripts are tree i , site j , and year t .

Covariate	Units	Data source
Diameter ($G_{ij,t}$, $G_{ij,t}^2$)	cm, cm ²	MASTIF
Crown class ($C_{ij,t}$)	ordinal (class 1-5)	MASTIF
Moisture surplus (S_j)	mm	terraClimate, CHELSA
Surplus anomaly ($S_{j,t}$)	mm	terraClimate, CHELSA
Temperature (T_j)	°C	terraClimate, CHELSA
Temperature anomaly ($T_{j,t}$)	°C	terraClimate, CHELSA
$S_j \times G_{ij,t}$	mm × cm	
CEC _{j} (0 - 30cm)	mmolc/kg	soilgrid250m
Slope, aspect (u_{1j} , u_{2j} , u_{3j})	radians	DEM, USGS

Table S3: Coefficients for climate effect on individual (ISP), community fecundity (CSP) and on NPP (MODIS or DGVMs TRENDY). ISP and CSP fecundity are fitted on a natural log scale. r^2 for ISP = 0.2, CSP = 0.15, NPP MODIS = 0.48, NPP DGVM = 0.52.

<i>Variable</i>	<i>Estimate</i>	<i>SE</i>	<i>P-value</i>
Climate effects on \log_e ISP			
<i>Intercept</i>	4.64e+00	4.93e-02	<2e-16
<i>T</i>	1.78e-01	6.01e-03	<2e-16
<i>T</i> ²	-5.60e-03	1.770e-04	<2e-16
<i>S</i>	-2.72e-03	4.80e-05	<2e-16
<i>S</i> ²	-1.12e-07	1.14e-08	<2e-16
<i>T</i> × <i>S</i>	1.84e-04	1.73e-06	<2e-16
Climate effects on \log_e CSP			
<i>Intercept</i>	9.88e+00	5.61e-01	<2e-16
<i>T</i>	9.96e-02	7.88e-02	0.21
<i>T</i> ²	-2.38e-03	2.82e-03	0.40
<i>S</i>	-9.21e-04	7.16e-04	0.20
<i>S</i> ²	2.87e-08	2.20e-07	0.90
<i>T</i> × <i>S</i>	1.19e-04	4.05e-05	3.60e-3
Climate effects on NPP (MODIS)			
<i>Intercept</i>	3.52e-01	2.46e-02	< 2e-16
<i>T</i>	1.54e-02	1.92e-03	5.18e-15
<i>S</i>	1.80e-04	3.34e-05	1.02e-07
<i>T</i> × <i>S</i>	1.12e-05	2.64e-06	2.41e-05
Climate effects on NPP (DGVMs TRENDY)			
<i>Intercept</i>	1.455e-01	2.2e-02	7.71e-11
<i>T</i>	3.19e-02	1.72e-03	< 2e-16
<i>S</i>	3.25e-04	3.00e-05	< 2e-16
<i>T</i> × <i>S</i>	-7.36e-06	2.38e-06	0.00199

670 **Supplementary Figures**

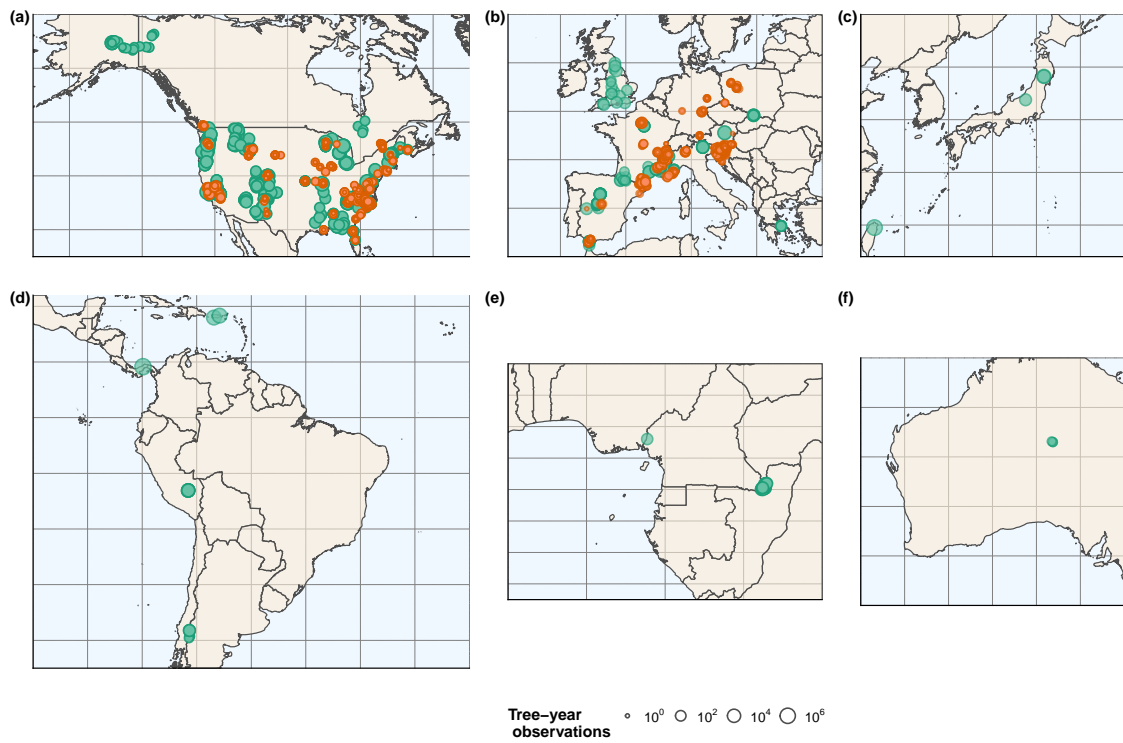


Figure S1: MASTIF data network, including longitudinal (green) and opportunistic (orange) observations in North America (a), Europe (b), Asia (c), South and Central America (d), Africa (e) and Oceania (f). Dot size represents the number of initial tree year observations at log10 scale. Numbers of observations are reported in Table S1.

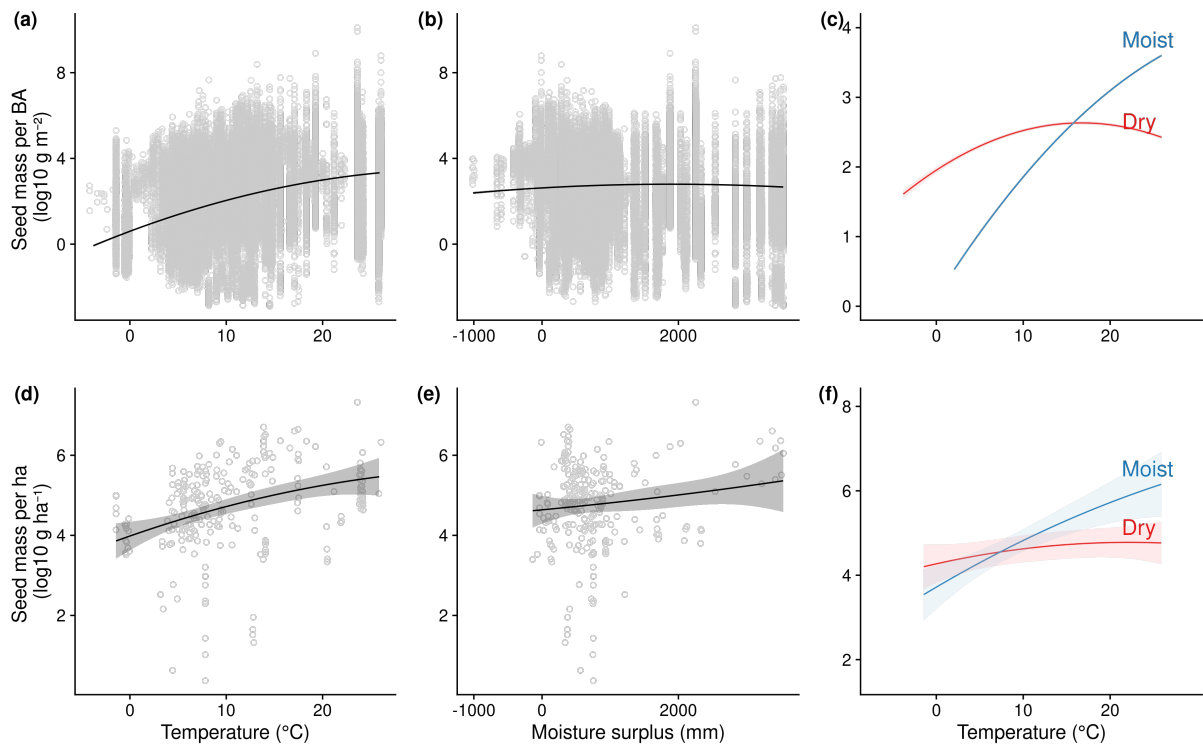


Figure S2: Climate responses for ISP (seed mass per basal area) (a, b, c) and stand-level CSP, as g ha^{-1} (d, e, f) showing marginal responses to temperature (a and d) and moisture surplus (d and e) with observations (dots) and the fitted model, and interactions between temperature and moisture surplus (c and f). Coefficients are reported in Table S3. Low and high values used for conditional plots in (c and f), labelled as Moist ($S = 1500 \text{ mm}$) and Dry ($S = -50 \text{ mm}$). Due to large sample size, confidence intervals around lines in (a, b, c) are not distinct from the predictive mean. Temperature and moisture surplus correspond here to a mean annual value for each sites.

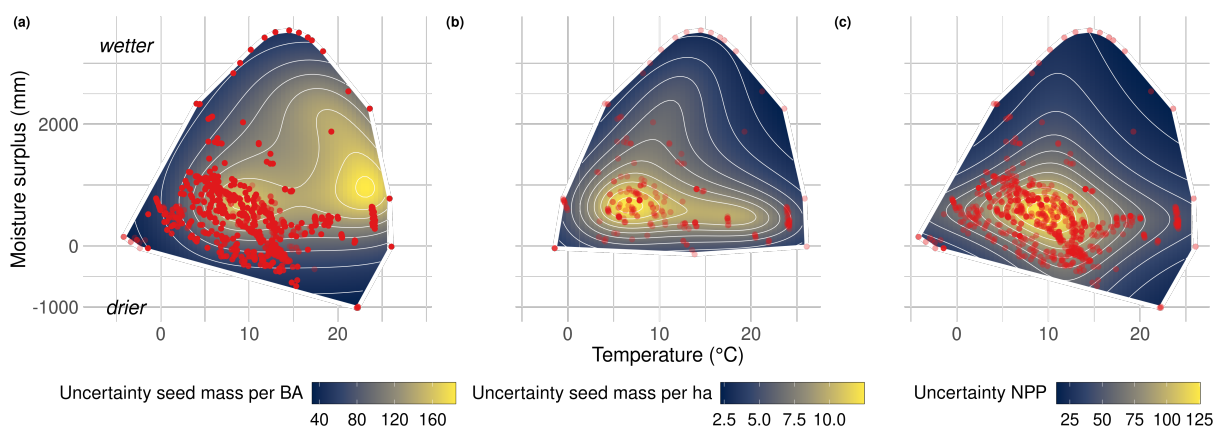


Figure S3: a) Uncertainty in the climate responses, defined as the inverse of the predictive standard error, for (a) ISP (seed production per tree basal area, $\text{log}_{10} \text{g m}^{-2} \text{y}^{-1}$) (b) CSP (seed production per ha forest floor, $\text{log}_{10} \text{g ha}^{-1} \text{y}^{-1}$), and (c) NPP ($\text{kg C m}^{-2} \text{y}^{-1}$). Convex hulls are defined by observations (red), including individual trees (a, c) and inventory plots (b). Surface scale color decreases as the inverse of the predictive standard error—blue edges reflect increased uncertainty at data extremes.

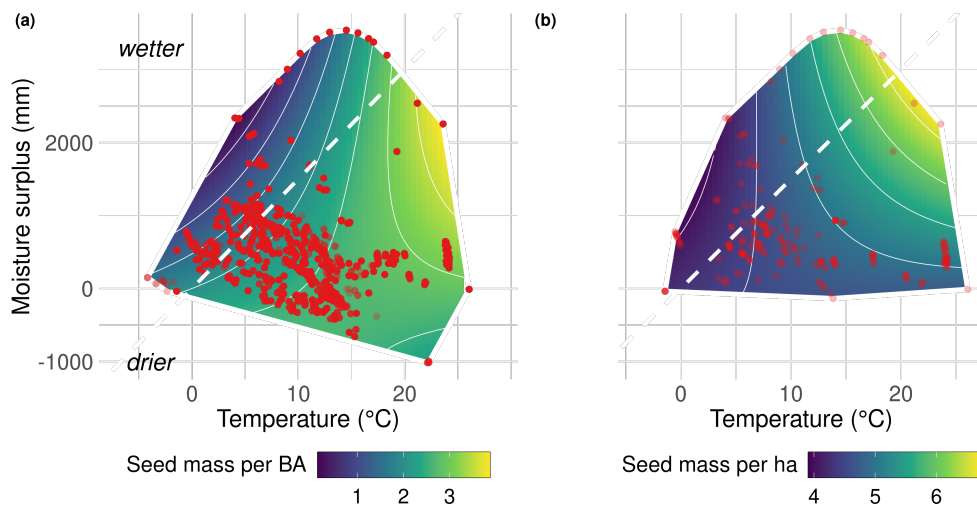


Figure S4: Because BCI includes the largest sample of tree years, we show that the same trend exists without BCI for both (a) ISP, (seed production per tree basal area, log₁₀ values) and (b) CSP (seed mass per ha forest floor, log₁₀ values).

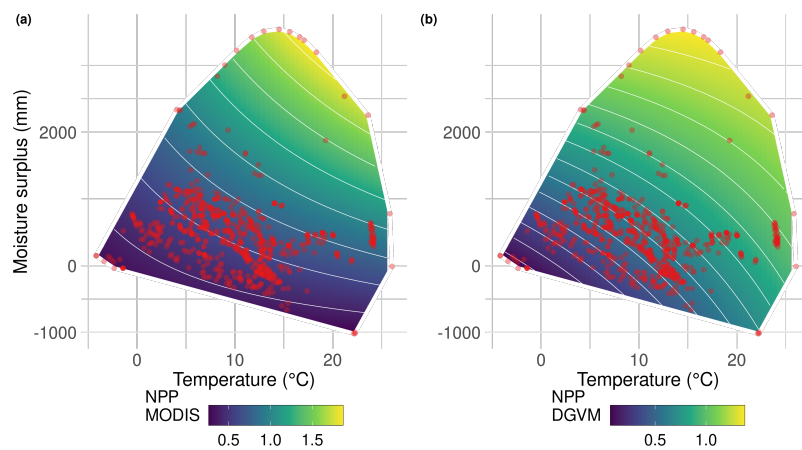


Figure S5: Climate response for NPP from MODIS (a) and the mean value from 11 DGVMs in TRENDY (b) show the same response to temperature.

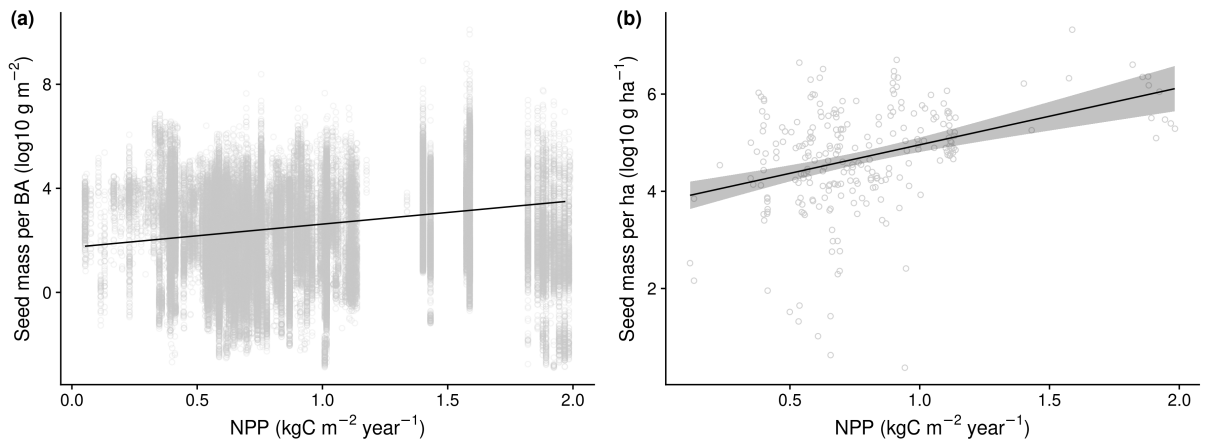


Figure S6: Relationships between NPP from MODIS and individual (standardized) fecundity ISP (a) and stand CSP (b), both positive ($p < 0.00001$) and both accounting for little of the variability ($r^2 = 0.05$ and 0.13 , respectively).

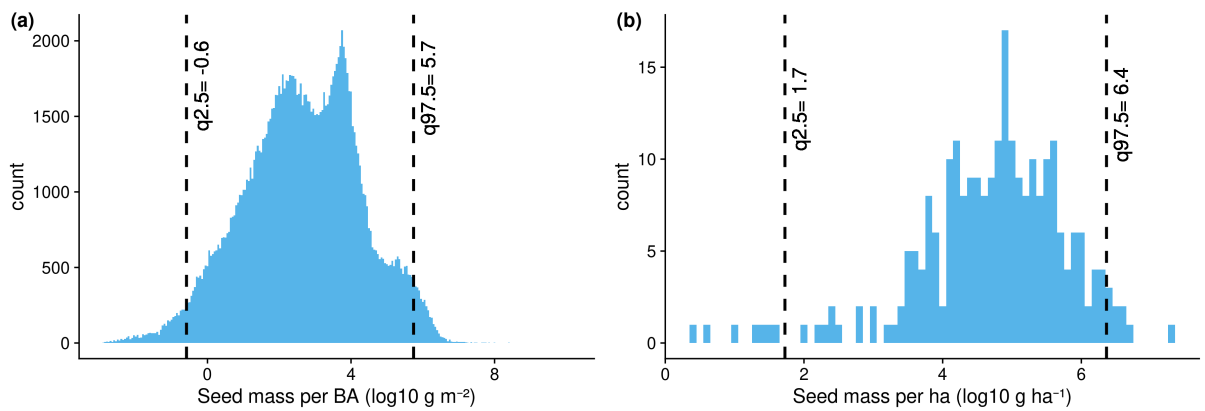


Figure S7: Distribution of (a) ISP (g seed per m² basal area) and (b) CSP (g seed per ha basal area) fecundities. Black dotted lines represent the quantile at 2.5 and 97.5%.